Journal of Alloys and Compounds 479 (2009) 855–858

Contents lists available at ScienceDirect

Journal of Alloys and Compounds

journal homepage: www.elsevier.com/locate/jallcom

Characterization of NiO nanoparticles by anodic arc plasma method

Zhiqiang Wei[a,b,*], Hongxia Qiao[c], Hua Yang[a], Cairong Zhang[a], Xiaoyan Yan[a]

[a] School of Science, Lanzhou University of Technology, Lanzhou, 730050, China
[b] State Key Laboratory of Advanced New Non-ferrous Materials, Lanzhou University of Technology, Lanzhou 730050, China
[c] School of Civil Engineering, Lanzhou University of Technology, Lanzhou, 730050, China

ARTICLE INFO

Article history:
Received 17 December 2008
Received in revised form 7 January 2009
Accepted 16 January 2009
Available online 31 January 2009

Keywords:
NiO nanoparticles
Anodic arc discharge
Particle size
Infrared absorption spectrum

ABSTRACT

NiO nanoparticles with average particle size of 25 nm were successfully prepared by anodic arc plasma method. The composition, morphology, crystal microstructure, specific surface area, infrared spectra, particle size distribution of product were analyzed by using X-ray diffraction (XRD), transmission electron microscopy (TEM) and the corresponding selected-area electron diffraction (SAED), Fourier transform infrared spectrum (FTIR) and Brunauer–Emmett–Teller (BET) N_2 adsorption. The experiment results shown that the NiO nanoparticles are bcc structure with spherical shape and well dispersed, the particle size distribution ranging from 15 nm to 45 nm with the average particle size is about 25 nm, and the specific surface area is 33 m^2/g.The infrared absorption band of NiO nanoparticles show blue-shifts compared with that of bulk NiO.

1. Introduction

Nanoparticles exhibit novel properties that significantly differ from those of corresponding bulk solid state owing to the different effects in terms of small size effect, surface effect, quantum size effect and macroscopic quantum tunnel effect [1,2]. In recent years, NiO nanoparticles as a kind of functional material has attracted extensive interests due to its novel optical, electronic, magnetic, thermal and mechanical properties and potential application in catalyst, battery electrodes, gas sensors, electrochemical films, photo-electronic devices, and so on [3–9]. In these applications, it is still needed for synthesizing high-quality and ultra-fine powders with required characteristics in terms of their size, morphology, microstructure, composition purity, crystallizability, etc. which are the most essential factors which eventually determine the microstructure and performance of the final products. Therefore, it is very important to control the powder properties during the preparation process.

There are many different methods reported for the synthesis of NiO nanoparticles, such as ultrasonic radiation, hydrothermal synthesis, carbonyl method, laser chemical method, pyrolysis by microwave, sol–gel method, precipitation–calcination, microemulsion method, and so forth [10–16]. However, to the best of our knowledge, most of the reported experimental techniques for the synthesis of nanopowders are still limited in laboratory scale due to some unresolved problems, such as special conditions, tedious procedures, complex apparatus, low-yield and high-cost. From a practical viewpoint, it is vital to develop a way to manufacture high-quality nanopowders at high throughput with low cost.

Anodic plasma method is an effective feasible process to prepare monodisperse metal nanopowders [17]. Compared with the conventional methods, anodic arc plasma method has many advantages: metal nanopowders prepared by this process with ultra-fine particle size, higher purity, and narrow size distribution, well-dispersed and spherical shape. Furthermore, the physical and chemical properties of the nanopowders can be easily controlled by varying the processing parameters and no need expensive agents or special equipment. In addition, it is a convenient, inexpensive process, has high productive capacity and the potential for further mass production in the industry.

In this paper, NiO nanoparticles were successfully prepared by anodic arc plasma technique. In addition, the composition, morphology, microstructure, specific surface area, infrared spectra, the particle size and distribution of product by this process were characterized via X-ray diffraction (XRD), transmission electron microscopy (TEM) and the corresponding selected-area electron diffraction (SAED), Fourier transform infrared spectrum (FTIR) and Brunauer–Emmett–Teller (BET) N_2 adsorption. The knowledge obtained would enhance a better understanding to the microstructure of NiO nanoparticles, and finally assist in the further development of novel properties and also benefit the practical industrial application in the future.

2. Experimental

The detailed experimental apparatus was fully illustrated elsewhere [17], it mainly include the stainless steel vacuum chamber, the gas supply device, the DC

* Corresponding author. Fax: +86 931 2976040.
E-mail address: zqwei7411@163.com (Z. Wei).

0925-8388/$ – see front matter © 2009 Elsevier B.V. All rights reserved.
doi:10.1016/j.jallcom.2009.01.064

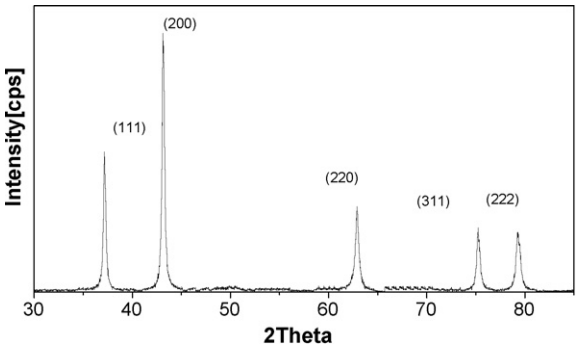

Fig. 1. XRD pattern of NiO nanoparticles.

power supply, the plasma generator with a high frequency initiator, the vacuum pump, the water-cooled collection cylinder and the water-cooled copper crucible. The bulk pure material to be evaporated was laid on the water-cooled copper crucible, which served as the anode. Ni rod with 10 mm diameter is mounted in an insulated and axial manner, which was also water-cooled and served as the cathode. In the process of preparation, the vacuum chamber was pumped to 10^{-3} Pa and then a mixture of O_2 and Ar (1:4 by volume ratio) were backfilled as a reactant gas to reach the desired pressure. The electric arc in the inert environment was automatically ignited between the Ni electrode and the nozzle by high frequency initiator, which was maintained by the current source at the pre-established values of the voltage and current. Under argon pressure and electric discharge current, the ionized gases were driven through the nozzle outlet and form the plasma jet. The bulk metal nickel (purity 99.99%) was heated and melted by the high temperature, and metal atom detached from the metal surface when the plasma jet kinetic energy exceeds the metal superficial energy, and evaporated into atom soot. Above the evaporation source was a region of supersaturated metal vapor, where metal atoms diffused around and collided with O atom to form NiO at high temperature due to the oxidation reaction. When the vapor was supersaturated, a new phase was nucleated homogeneously out of the aerosol systems. The droplets were rapidly cooled and combined to form primary particles by an aggregation growth mechanism. The particles were transported from the nucleation and growth region to the inner walls of the cylinder by the free inert gas convection between the hot evaporation source and the cooled collection cylinder, the loose nanoparticles could be obtained.

The crystalline structures of the products were characterized by a rotating-target X-ray diffractometer (Japan Rigaku D/Max-2400) equipped with a monochromatic high-intensity Cu Kα radiation (λ = 1.54056 Å, 40 kV, 100 mA), The sample was scanned in a range from 30° to 90° (2θ) with scanning rate was 0.005°/s and step size 0.02°. The average crystalline grain size of the NiO nanoparticles was estimated from the half maximum width and the peak position of an XRD line broadened according the Scherrer formula, which was further confirmed by the transmission electron microscopy (TEM) results and BET results.

The particle size and morphology of the sample and the corresponding selected-area electron diffraction (SAED) were examined by JEOL JEM-1200EX transmission electron microscopy (TEM) with an accelerating voltage of 80 kV. In the process of preparation of the TEM specimen, a small amount of the powders was dispersed in a few milliliters of ethanol in an ultrasonic bath and ultrasonic treated for 30 min, and a drop from an eye dropper of the resulting suspension were placed onto a carbon coated copper grid. The samples were placed in a vacuum oven to dry at ambient temperature before examining. The sample is scanned in all zones before the picture is taken.

The specific surface area of the sample was calculated from the BET adsorption equation and measured by the accelerated surface area porosimetry (ASAP 2010) instrument produced by Micromerities Corp at liquid nitrogen temperature (78 K).

The absorption spectroscopy spectra of the product were recorded from 400 cm^{-1} to 4000 cm^{-1} on a Nicolet Nexus 670 Fourier transforms infrared (FTIR) spectrometer using the KBr pellet technique to determine the chemical structure of the sample.

3. Results and discussion

The purity and crystallinity of the as-synthesized NiO nanoparticles were examined by using powder X-ray diffraction (XRD) as shown in Fig. 1. It can be seen from Fig. 1 that the diffraction peaks are low and broad due to the small size effect and incomplete inner structure of the particle. The peaks positions appearing at $2\theta = 37.20°, 43.20°, 62.87°, 75.20°$ and $79.38°$ can be readily indexed as (1 1 1), (2 0 0), (2 2 0), (3 1 1), and (2 2 2) crystal planes of the bulk NiO, respectively. All these diffraction peaks can be perfectly indexed to the face centered cubic (FCC) crystalline structure of NiO, not only in peak position, but also in their relative intensity of the characteristic peaks, which is in accordance with that of the standard spectrum (JCPDS, No. 04-0835). The XRD pattern shows that the samples are single-phase and no any other impurities distinct diffraction peak except the characteristic peaks of FCC phase NiO was detected. This result shows that the physical phases of the NiO nanoparticles have higher purity prepared in this work. The NiO lattice constant calculated from the XRD data is 4.1729 Å, which is in good agreement with the reported data (JCPDS 4-835).

The average crystallite size is calculated by X-ray diffraction line broadening using the Scherrer formula: $d = \frac{K\lambda}{B\cos\theta}$, where d represents the grain size; $K = 0.89$ is the Scherrer constant related to the shape and index (hkl) of the crystals; λ is the wavelength of the X-ray (Cu Kα, 1.54056 Å,); θ is the diffraction angle of the peak; and B stands for the full-width at half-height of the peaks (in radian) given by $B^2 = Bm^2 - Bs^2$, where Bm is the full-width at half maximum (FWHM) of the sample and Bs is the half-width of a standard sample with a known crystal size greater than 100 nm, the effect of instrumental broadening on the reflection peaks is calibrated. The crystallite sizes of NiO samples is 23 nm which was calculated from measured values for the spacing of the (1 1 1) plane.

Fig. 2(a) shows the representative transmission electron microscopy image of NiO nanoparticles. TEM analysis of the products provided information on the size and morphology of NiO

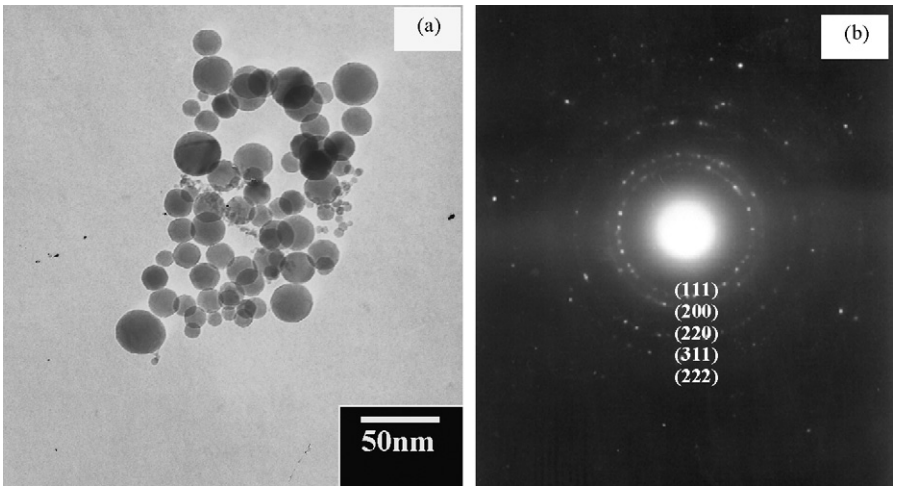

Fig. 2. (a) TEM micrograph and (b) the selected-area electron diffraction pattern of NiO nanoparticles.

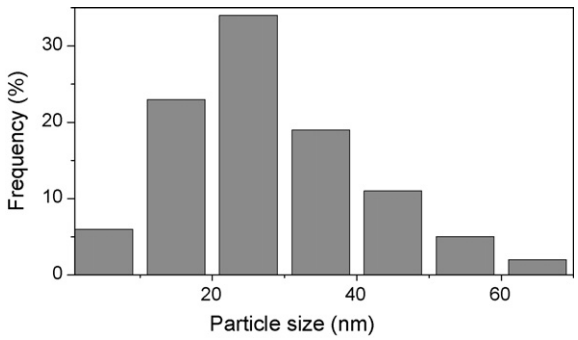

Fig. 3. Particle size distribution of NiO nanoparticles.

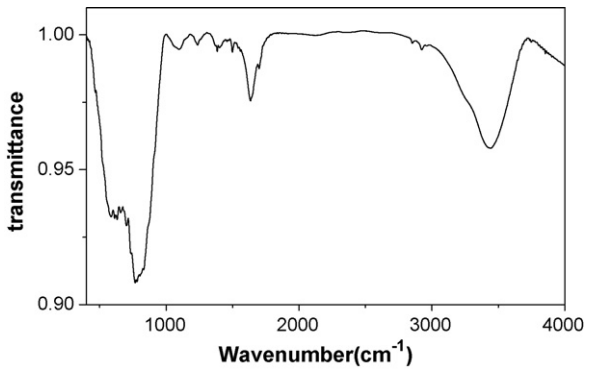

Fig. 5. FTIR spectra of NiO nanoparticles.

nanoparticles and their state of agglomeration. It can be seen from Fig. 2(a) that the NiO nanoparticles had spherical shapes and were well dispersed with smooth surface and uniform size. Few small particles aggregate into secondary particles because of their extremely small dimensions and high surface energy.

Fig. 2(b) shows the corresponding selected-area electron diffraction (SAED) pattern. The SAED pattern consists of five diffraction rings with different radius and one centre. The diameter of the diffraction ring in SAD pattern is proportional to $\sqrt{h^2+k^2+l^2}$ where (*hkl*) are the Miller indices of the planes corresponding to the ring, counting from the centre 1st, 2nd, 3rd, 4th and 5th rings correspond to (1 1 1), (2 0 0), (2 2 0), (3 1 1) and (2 2 2) planes respectively. Tropism of the particles at random and small particles cause the widening of diffraction rings that made up of many diffraction spots, which indicates that the nanoparticles are polycrystalline structure. The SAED pattern also confirms that the NiO nanoparticles is face centered cubic (FCC) structure NiO in crystallography, which consistent with the above X-ray result.

From the data obtained by TEM micrographs, the particle size histograms can be drawn and the mean size of the particles can be determined. Fig. 3 shows the particle size distribution of NiO nanoparticles. It can be seen that the particle sizes possess a small and narrow size distribution in a range from 15 nm to 45 nm, and the mean diameter (taken as average particle diameter) is about 25 nm. We notice that the mean particle size determined by TEM is in good agreement with the average crystallite size calculated by Scherer formula from the XRD patterns. According to the TEM image, it could be concluded that this preparation method had successfully overcome the problem of agglomeration and appropriate to obtain the NiO nanoparticles with smaller crystalline size.

The surface area analysis was carried out on NiO nanoparticles by BET method. Assuming the particles possess solid, spherical shape with smooth surface and same size, the surface area can be related to the average equivalent particle size by the equation: $D_{BET} = 6000/(\rho\, S_w)$ (in nm), where D_{BET} is the average diameter of a spherical particle; S_w represents the measured surface area of the powder in m^2/g; and ρ is the theoretical density in g/cm^3. Fig. 4 shows BET plots of NiO nanoparticles, the specific surface area of NiO nanoparticles calculated using the multi-point BET-equation is 33 m^2/g, and the calculated average equivalent particle size is 28 nm. We noticed that the particle size obtained from the BET and the TEM methods, agree very well with the result given by X-ray line broadening. The results of TEM observations and BET methods further confirmed and verified the relevant results obtained by XRD as mentioned above.

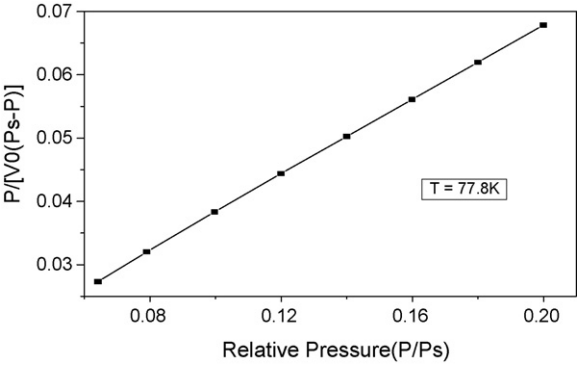

Fig. 4. BET plots of NiO nanoparticles.

Fig. 5 shows the FTIR spectra of NiO nanoparticles, which showed several significant absorption peaks. The broad absorption band in the region of 600–700 cm^{-1} is assigned to Ni—O stretching vibration mode, the broadness of the absorption band indicates that the NiO powders are nanocrystals. The size of samples used in this study was much less than the bulks form NiO, so that NiO nanoparticles had its IR peak of Ni—O stretching vibration and shifted to blue direction. If a light quantum is absorbed in NiO, an electron is transferred from the valence band into the conduction band, leaving behind a positive hole. In small particles, the wave functions of the electron and the hole are confined to the particle volume. Hence, if the particle size becomes comparable or smaller than the de Broglie wave length of the charge carriers, the confinement increases the energy required for creating an electron/hole pair. This increase shifts the absorption/luminescence spectra towards shorter wave lengths (blue). Due to their quantum size effect and spherical nanostructures, the FTIR absorption of NiO nanoparticles is blue shifted compared to that of the bulk form.

Besides the Ni—O vibration, it could be seen from Fig. 5 that the broad absorption band centered at 3440 cm^{-1} is attributable to the band O—H stretching vibrations and the weak band near 1635 cm^{-1} is assigned to H–O–H bending vibrations mode were also presented, due to the adsorption of water in air when FTIR sample disks were prepared in an open air. These observations provided the evidence to the effect of hydration in the structure. Meanwhile, it implied the presence of hydroxyl in the precursor, and the broad absorption around 767 cm^{-1} is assigned to the band C=O stretching vibrations, The serrated absorption bands in the region of 1000–1500 cm^{-1} are assigned to the O—C=O symmetric and asymmetric stretching vibration and the C—O stretching vibration, but the intensity of the band has weakened, which indicated that the ultra-fine powers tend to strong physically absorption to H_2O and CO_2.

4. Conclusions

Cubic NiO nanoparticles with spherical shape higher purity, well-dispersed and narrow size distribution ranges from 15 to 65 nm were successfully prepared by anodic arc plasma method

and different approaches such as XRD, TEM, SAED, FTIR and BET were used to characterize.

The specific surface area of the sample is 33 m^2/g calculated from the BET adsorption equation, the average particle size about 25 nm, the average equivalent particle size obtained from the TEM and confirmed by XRD and BET results. The infrared absorption band of the NiO nanoparticles show blue-shifts compared with that of bulk NiO.

Acknowledgements

This work was supported by the Key Project of Chinese Ministry of Education (No.208151), Natural Science Foundation of Gansu Province, China (No.2007GS04821) and Scientific Research Developmental Foundation of Lanzhou University of Technology (No. SB10200805)

References

[1] H. Gleiter, Nanocrystalline materials, Prog. Mater. Sci. 33 (4) (1990) 223.
[2] Z.L. Wang, Y. Liu, Z. Zhang, Handbook of nanophase and nanostructed materials, Tsinghua University Press, 2002.
[3] F. Takehia, O. Satoshi, O. Hajime, et al., Properties of NiO cathode coated with lithiated Co and Ni solid solution oxide for MCFCS, J. Power Sources 86 (2001) 340.
[4] I. Yoshiyuki, M. Yoshihiro, T. Watanabe, et al., Direct observation of the oxidation nickel in molten carbonate, J. Power Sources 75 (2) (1998) 236.
[5] I. Hotovy, J. Huran, L. Spiess, et al., Preparation of nickel oxide thin films for gas sensors applications, Sens. Actuators B 57 (1999) 147.
[6] H. Bi, S.D. Li, Y.C. Zhang, Ferromagnetic like behavior of ultrafine NiO nanocrystallites, J. Magn. Magn. Mater. 277 (3) (2004) 363.
[7] Y. Ichiyanagi, N. Wakabayashi, J. Yamazaki, et al., Magnetic properties of NiO nanopardcles, Phys. B: Condens. Matter (2003) 862, 329-333.
[8] V. Biju, M. Abdul Khadar, Fourier transform infrared spectroscopy study of nanostructured nickel oxide, Spectrochim. Acta Part A: Mol. Biomol. Spectrosc. 59 (1) (2003) 121.
[9] G.Z. Wang, L.D. Zhang, J.M. Mou, Preparation and optical absorption of nanometer NiO particles, Acta Phys. Chim. 13 (5) (1997) 445.
[10] S.W. Wang, X.K. Chen, Preparation of fine particles by method of laser chemistry-preparation of nickel series particles, Chinese J. Laser 16 (12) (1989) 741.
[11] W. Yan, J.J. KE, Preparation of nickel oxide particles by decomposition of basic nickel carbonate in microwave absorbing additive, Mater. Rev. Bull. 31 (1) (1996) 51.
[12] S.L. Che, K. Takada, Preparation of dense spherical Ni particles and hollow NiO particles by spray pyrolysis, J. Mater. Sci. 34 (1999) 1313.
[13] J.L. Katz, P.F. Miquel, Synthesis and applications of oxides and mixed oxides produced by a flame process, Nanostruct. Mater. 4 (5) (1994) 551.
[14] Y.D. Li, C.W. Li, X.F. Duan, et al., Preparation of nanocrystalline NiO in mixed solvent, J. China Univ. Sci. Tech. 27 (3) (1997) 346.
[15] W.Z. Wang, Y.K. Liu, C.K. Xu, et al., Synthesis of NiO nanorods by a novel simple precursor thermal decomposition approach, Chem. Phys. Lett. 362 (1-2) (2002) 119.
[16] L. Xing, X.Y. Deng, Y. Jin, Experimental study on synthesis of NiO nanoparticles, Scripta Mater. 47 (2002) 219.
[17] Z.Q. Wei, T.D. Xia, L.F. Bai, et al., Efficient preparation for Ni nanopowders by anodic arc plasma, Mater. Lett. 60 (3) (2006) 766.